Deformation Mechanism of Thermoplastic Two-Phase Elastomers of Lamellar Morphology Having a High Volume Fraction of Rubbery Microphase

R. Séguéla and J. Prud'homme*

Department of Chemistry, University of Montreal, Montreal, Quebec, Canada H3C 3V1.
Received July 28, 1980

ABSTRACT: Thermoplastic two-phase elastomers exhibiting a lamellar morphology have been obtained by solvent casting a polybutadiene-hydrogenated SBS block polymer (SBS-H) having a styrene weight fraction of 0.29 only. The deformation mechanism of the SBS-H specimens, which consisted of randomly oriented stacks of alternating glassy and rubbery lamellae, has been investigated by small-angle X-ray scattering (SAXS) combined with local strain measurements. Particular attention has been paid to the neck deformation process which occurred upon the first stretching. Local strain measurements carried out through the neck region indicated a postyield isotropic constant-volume deformation. Concurrent SAXS studies showed orientation and shear of lamellar grains at an angle close to 20° with respect to the stretching direction, both being reversible processes. Also observed was an affine deformation of the rubbery chains in the oriented and sheared grains. It is shown that these observations can be rationalized by considering the yielded material as a dispersion of discrete microcomposite lamellar entities which follow the lowest energy path of rearrangement in response to the uniaxial macroscopic deformation.

Introduction

Thermoplastic two-phase elastomers have received considerable interest in recent years. Among these materials, much attention has been given to poly(styrene-*b*-butadiene-*b*-styrene) (SBS) and poly(styrene-*b*-isoprene-*b*-styrene) (SIS) three-block polymers.[1] The influence of their morphology on their mechanical properties has been thoroughly investigated by means of electron microscopy and small-angle X-ray scattering (SAXS). Generally, solvent-cast specimens of SBS or SIS polymers having styrene contents in the range of about 15–30% by weight exhibit high elasticity with stress softening upon repeated extensions.[2,3] This latter phenomenon, which is similar to the Mullins effect in reinforced rubbers, has been attributed to ductile deformation or rupture of the glassy PS microdomains, which appear in the form of spheres, strings of pearls, or short rods dispersed in the rubbery phase. At higher styrene contents (30–60%), solvent-cast specimens of SBS or SIS generally exhibit yield point and neck propagation upon first stretching, while high elasticity and stress softening occur upon subsequent extensions.[2,4,5] At these higher styrene contents the PS microdomains take the form of parallel long rods or lamellae which undergo rupture at the yield point. It has also been found that the morphology of SBS or SIS polymers and related polydiene-hydrogenated compounds can be affected by the nature of the casting solvent.[6,7] This effect appears to be particularly pronounced for systems having styrene contents in the range of about 20–40% by weight, for which good solvents for polystyrene give more continuous PS microdomains than selective solvents for the rubbery material.

In addition to rupture of the glassy microdomains, other microscopic structural changes occur upon first extension of thermoplastic two-phase elastomers having rodlike or lamellar morphology. These are bending, kinking, and shearing of the glassy rods or lamellae.[5,8] Since solvent-cast specimens often show randomly oriented grains (i.e., highly ordered regions) such as arrays of parallel rods or stacks of parallel lamellae, it is reasonable to expect that during neck propagation and further extension of the specimen these grains will undergo rotation and shear as a whole. In fact, such effects have been observed by Daniewska and Picot[9] for both SBS and SIS specimens having rodlike morphologies. The deformation mechanism of a lamellar SBS system having a styrene weight fraction of 0.48 has been extensively studied by Hashimoto et al.[5] According to these authors, the necking process involved zigzag bending and inclination of the PS lamellae toward the stretching direction. Their evidence for inclination of the PS lamellae was based on the buildup of a SAXS four-point pattern after the yield point in moderately stretched specimens. They also showed electron micrographs displaying chevron textures when taken on stretched specimens stained (and hardened) by OsO_4.

In a previous paper[7] we reported a study in which a polybutadiene-hydrogenated SBS block polymer (hereafter designated as sample SBS-H) having a styrene weight fraction as low as 0.29 presented a lamellar two-phase structure when cast from toluene solution at room temperature. The well-defined morphology of the sample was founded on its SAXS pattern, which showed the first six scattering maxima expected for a lamellar spacing of 33.2 nm. Also reported in the previous paper[7] was the stress–strain behavior of the SBS-H specimen cast from toluene solution. Its behavior was similar to those already described for SBS or SIS block polymers having a lamellar morphology. The SBS-H specimen exhibited yield point and neck propagation upon first stretching and stress softening upon subsequent extension cycles.

In the present paper we report a detailed SAXS study of the structural changes produced in the region of the neck, at different local strains, for the SBS-H lamellar system. A particularity of the present system was the much larger volume fraction of the rubbery microphase (75%) when compared to that (~50%) of the SBS sample studied by Hashimoto et al.[5] This large difference between the volume fractions of the two microphases in the SBS-H lamellar system allowed the observation of the second-order diffraction maximum, which, due to the extinction rules for a lamellar structure,[10] was not observed in the SBS sample of 1:1 composition studied by Hashimoto et al. Another feature of the present SBS-H system which results from the larger volume fraction of the rubbery microphase was its ability to almost completely recover its original lamellar packing in a few minutes, at room temperature, after stretching to high elongation.

Experimental Section

Material. The polybutadiene-hydrogenated SBS block polymer designated as SBS-H was a commercial polymer man-

0024-9297/81/2214-0197$01.00/0

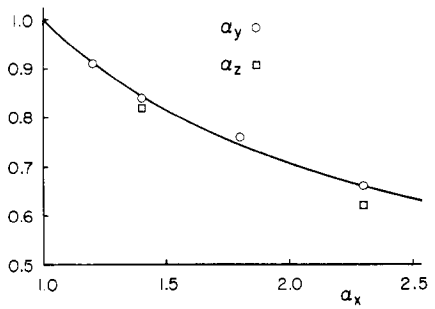

Figure 1. Variation of the local contraction ratios α_y and α_z measured in the neck region along the width and the thickness of the specimen, respectively, as a function of the longitudinal local draw ratio α_x. The curve represents the theoretical variation ($\alpha_y = \alpha_z = \alpha_x^{-1/2}$) expected for an isotropic deformation at constant volume.

ufactured by Shell Chemical Co. under the trade name Kraton GX-6500. Its molecular characteristics[7] were $M_n = 6.9 \times 10^4$ and styrene weight fraction $w_s = 0.29$. NMR analysis[7] indicated that the polybutadiene-hydrogenated midblock was quite similar to a random copolymer of ethylene and 1-butene having an ethylene molar content close to 78%. This latter polyolefinic block was perfectly amorphous and rubbery at room temperature.

Film Preparation. The SBS-H sample was cast into films from 5% toluene solution on a mercury surface. The solvent was slowly evaporated at room temperature over a period of 3–4 days. The cast films were subsequently dried under high vacuum for at least 1 week. Their thickness was about 0.8 mm. Test pieces for SAXS and mechanical measurements were cut into rectangular strips 3-cm long and 0.5-cm wide.

Small-Angle X-ray Scattering (SAXS) and Local Strain Measurements. The SAXS study was performed in the photographic mode on a Model 2202 Rigaku-Denki goniometer provided with a two-pinhole collimator. Nickel-filtered Cu Kα radiation ($\lambda = 0.154$ nm) was generated by a Philips tube operating at 40 kV and 20 mA. The second pinhole, specimen, and photographic film were, respectively, placed at 300, 320, and 630 mm from the first pinhole. The diameters of the first and the second pinholes were 0.3 and 0.2 mm, respectively, for the recordings of the first-order diffraction. All other patterns were recorded with pinholes of 0.5 and 0.3 mm, respectively. For each order, exposure time was increased inversely to the thickness of the sample in order to balance the decrease of scattering volume upon stretching. The SAXS patterns associated with different stages of deformation along the neck region were issued from the same place of a film specimen, owing to a stepwise-controlled propagation of the neck. The X-ray beam impingement was centered into a square ink mark which allowed the measurements of the longitudinal and transversal local strains characterizing each stage of deformation along the neck region. This reference square mark was about 1 × 1 mm prior to deformation. The local strain perpendicular to the film surface was also measured in the region of the mark. Local strains at various angles with respect to the stretching direction were measured by using a circular ink mark of 1-mm diameter drawn on another specimen of the same dimensions. All local strains were measured with a microscope.

Results and Discussion

(a) Macroscopic Behavior. The yield behavior and plasticlike deformation of the lamellar SBS-H specimen started with the formation of a single neck at very low longitudinal draw ratio, $\alpha_x = 1.05$, and proceeded through the propagation of two neck regions in opposite directions. The length of each neck region was about 5 mm. The highest value of the local draw ratio α_x measured in the neck region was close to 2.3, indicating a large gradient of local strain all along the neck region. Figure 1 shows the variation of the local contraction ratios α_y and α_z measured along the width and the thickness of the specimen, respectively, as functions of the longitudinal local draw ratio α_x. From Figure 1 it may be seen that both α_y and α_z are

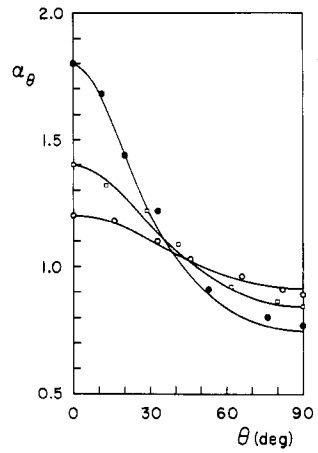

Figure 2. Variation of the local draw ratio α_θ measured in the plane of the film specimen, in the neck region, as a function of angle θ to the stretching direction. Shown are data points for local draw ratios $\alpha_x = 1.2$ (○), 1.4 (□), and 1.8 (●) together with the corresponding theoretical curves predicted by eq 1 for an isotropic deformation at constant volume.

close to the theoretical curve ($\alpha_y = \alpha_z = \alpha_x^{-1/2}$) expected for an isotropic deformation at constant volume. This behavior suggests that the neck deformation proceeds mainly through local extension and contraction of the rubbery microphase with little ductile deformation of the glassy microphase.

Figure 2 shows the variation of the local draw ratio α_θ measured in the plane of the specimen at different angles θ with respect to the stretching direction for three different values of the longitudinal local draw ratio ($\alpha_x = 1.2$, 1.4, and 1.8). Also shown on Figure 2 are the corresponding theoretical curves calculated assuming a constant-volume isotropic deformation of the material. The theoretical curves were computed by the relation

$$\alpha_\theta = [\alpha_x^2/(\alpha_x^3 \sin^2\theta + \cos^2\theta)]^{1/2} \quad (1)$$

which can be derived by considering the constant-volume uniaxial deformation of a unit sphere to an ellipsoid of revolution about the axis of stretch, x. This is the well-known strain ellipsoid model for a uniaxial tensile deformation. From the data in Figure 2 one can see that the angular dependence of the local strain is also in good agreement with the theoretical curves predicted for an isotropic constant-volume deformation. The results displayed in Figure 2 provide a more detailed description of the macroscopic deformation in the neck region than those in Figure 1. They show that the zero-strain direction decreases slightly from 51 to 42° as the longitudinal local draw ratio α_x increases from 1.2 to 1.8. As will be shown in the next section, the SAXS study of the neck region in the same range of α_x indicates the prevalence of lamellar diffracting grains with their PS lamellae oriented at an angle near to 20° with respect to the stretching direction. Also in the next section, it will be shown that the deformation of the diffracting grains in the neck region is insufficient to account for the macroscopic deformation of the specimen. Both these behaviors, i.e., the microscopic orientation of the lamellar grains being far from the zero-strain macroscopic direction and the nonaffine deformation of the grains, suggest that the plasticlike deformation occurring in the neck region is associated with at least two types of structural rearrangements. Our interpretation is that one type of rearrangement is associated with the disruption of the continuous PS microphase in areas which spread within the plane of any cross section of the specimen. This disruption process would occur at

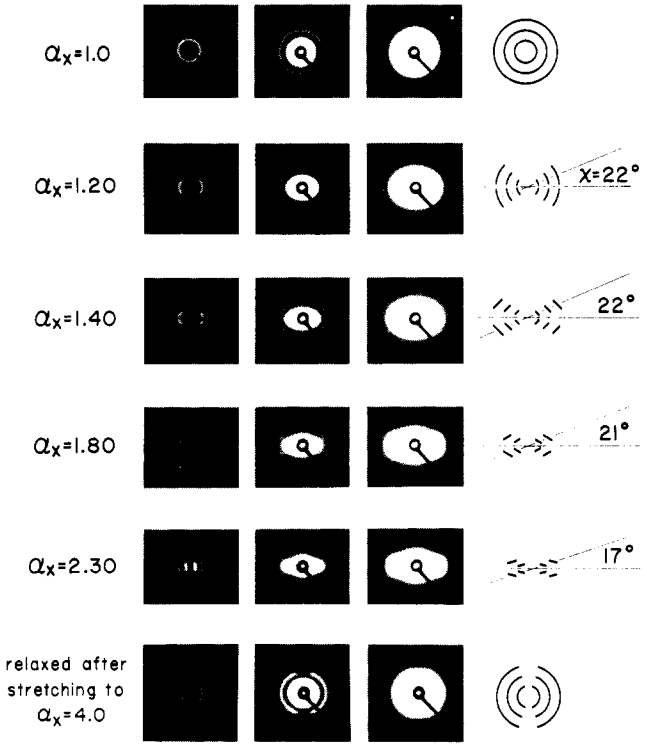

Figure 3. SAXS patterns recorded for different local draw ratios α_x of the neck with increasing exposure time from the left to the right. Also shown at the bottom is the SAXS pattern of a specimen allowed to retract after stretching to $\alpha_x = 4$. The stretching direction is vertical.

the yield point and would rapidly result in a homogeneous dispersion of lamellar grains in a mechanically isotropic disrupted medium. The grain sizes would be sufficiently small not to affect the macroscopic rubberlike behavior resulting from the deformation of the disrupted continuous medium. The other type of rearrangement would be associated with the microscopic orientation and deformation of the lamellar grains resulting from the large strain of the disrupted medium.

(b) Microscopic Behavior. Figure 3 shows the evolution of the diffraction maxima of the first three orders in SAXS patterns recorded for different local draw ratios (α_x = 1.2, 1.4, 1.8, and 2.3) in the neck region. The main feature of each diffraction order is a four-point diagram similar to those currently observed in SAXS patterns of drawn crystalline polymers.[11-13] From Figure 3 one can see that the four-point diagrams begin to appear at α_x = 1.2 and remain until α_x = 2.3, where the necking process is nearly complete. One can also see that the four-point diagram angle χ (see Figure 3) is close to 20° from α_x = 1.2 to α_x = 2.3. This means that over the whole necking region a large number of stacked lamellae remain oriented with an axial symmetry at an angle χ with respect to the stretching direction. In spite of the large gradient of local strain along the neck, this orientation appears to move little, contrary to what is observed for crystalline polymers in the same range of strain.[13] On the other hand, inspection of Figure 3 shows that the elongated diffraction lobes in the four-point diagrams rotate toward the direction perpendicular to the stretching direction when α_x increases from 1.2 to 2.3. This latter fact together with the preceding feature concerning the nearly constant four-point angle χ can be interpreted as a change of the grain orientation without a significant change of the lamellar orientation. This suggests an intragrain shearing process in which the stacking axis of the diffracting grains becomes oriented

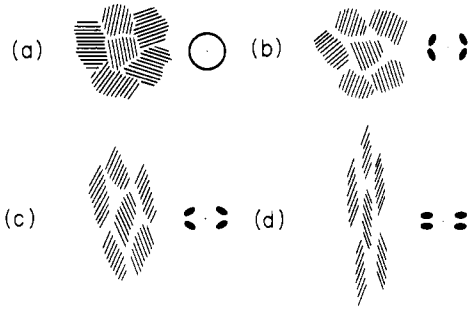

Figure 4. Schematic description of the grain arrangement at different stages of neck deformation together with the corresponding first-order diffraction maxima. Stretching direction vertical. For details see text.

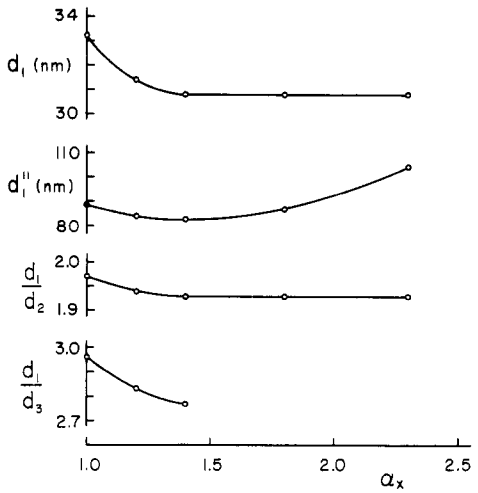

Figure 5. Variation of the first-order Bragg spacing d_1, the period d_1'' parallel to the stretching direction, and the ratios d_1/d_2 and d_1/d_3 of the first-order to the second- and third-order spacings as functions of the local draw ratio α_x in the neck region.

along the stretching direction.

A schematic description of the structural modifications of the diffracting grains is presented in Figure 4. Only shown in Figure 4 are grains of parallel lamellae able to produce each of the SAXS patterns displayed in Figure 3. Before stretching, the material consists of randomly oriented regions of parallel lamellae (Figure 4a). At the beginning of the necking process, i.e., at α_x = 1.2, the diffracting entities are mainly grains whose lamellae show a prevalent orientation close to 22° with respect to the stretching direction. This means that the other grains have either lost their regular spacing or undergone rotation toward the prevalent orientation. At this stage (Figure 4b), the stacking axis of the diffracting grains remains nearly normal to the lamellar surfaces. Then a progressive static shear of each grain brings their stacking axis close to the stretching direction (Figure 4c through Figure 4d). This enables longitudinal extension together with lateral contraction of the grains without a significant change of their lamellar orientation. At the end of the necking process (Figure 4d), the material is characterized by elongated stacks of tilted parallel lamellae which form a fiberlike chevron structure. This latter picture is in good agreement with the electron micrograph shown by Hashimoto et al.[5] for an ultrathin section of their SBS film specimen stretched to α_x = 1.8. Note that the ability of a fiberlike lamellar structure such as that represented in Figure 4d to generate a four-point diffraction pattern with lobes elongated in the direction perpendicular to the fiber axis has already been demonstrated by optical analogue studies

in the context of plastic deformation of crystalline polymers.[11,12]

Figure 5 shows the relation between the Bragg spacing d_1 of the first-order diffraction maximum and the local draw ratio α_x. Also shown in Figure 5 are the variation of the period d_1'' parallel to the stretching direction, and the variation of the ratios d_1/d_2 and d_1/d_3 of the first-order to the second- and third-order spacings, respectively. From Figure 5 one can see that the spacing d_1, which is that perpendicular to the lamellar surfaces, decreases slightly from 33.2 nm at $\alpha_x = 1.0$ to 30.8 nm at $\alpha_x = 1.4$ and remains at this latter value until $\alpha_x = 2.3$. Concurrently, the period d_1'' very slightly decreases until $\alpha_x = 1.4$, after which it increases from 82 to 104 nm. Note that $d_1'' = d_1/\sin\chi$, where χ is the angle between the lamellar surfaces and the stretching direction. These changes of the periods d_1 and d_1'' with increasing α_x in the neck region indicate a first stage at $\alpha_x < 1.4$ in which the rubbery lamellae in the diffracting grains are slightly compressed at a nearly constant inclination of 22° with respect to the stretching direction followed by a second stage at $\alpha_x > 1.4$ in which the inclination gradually decreases to 18° without any further compression of the rubbery lamellae. This latter stage corresponds to the static shear deformation of the grains described above.

As mentioned in the former section, the necking process is induced by the disruption of the PS microphase in areas which spread within the plane perpendicular to the stretching direction. The stress threshold for this process is the yield point before which any deformation is perfectly elastic and reversible. When the applied stress reaches the yield point, the disruption process occurs in an unforeseeable position and a neck appears. Due to the decrease of the cross section at the location of the neck, the increase of the true stress promotes subsequent disruption of the PS microphase in the regions close to both fronts of the neck. Hence only one neck generally forms and propagates over the whole length of the specimen. Distortion and rupture of the PS microphase should occur principally in the less ordered boundary regions between adjoining stacks and in stacks whose PS lamellae are far from the prevalent orientation observed for $\alpha_x > 1.2$. From the bottom of Figure 3 one can see that the SAXS pattern of a specimen relaxed at room temperature for a few minutes after stretching to $\alpha_x = 4$, i.e., well above the point of necking completion, is almost identical with that recorded before stretching. However, the meridian diffraction is absent in the pattern of the relaxed specimen. This indicates that the more severely disrupted or distorted regions were those with PS lamellae perpendicular to the stretching direction.

The preservation of several diffraction orders of the four-point type all along the neck region and the recovery of the original isotropic diffraction pattern after relaxation at room temperature indicate that a good many grains remained whole and retained their lamellar packing all along the neck deformation. In this regard, the departure of the spacing ratios d_1/d_2 and d_1/d_3 from the expected integer values of 2 and 3 as shown in Figure 5 is not at all in contradiction with the lamellar packing. Indeed, Reinhold et al.[14] showed that a dissymmetric distribution of the lamellar thicknesses may shift the SAXS maxima in such a way that the spacing ratios may deviate from the expected integer values. It seems that the shearing process induces a negative dissymmetry in the distribution of the lamellar thicknesses, presumably due to an uneven compression of the rubbery lamellae.

The driving force for orientation and shear of the nondisrupted stacks during the necking process lies in the hindrance of their rigid PS lamellae to the stress-induced macroscopic deformation of the material. In fact, the processes observed by SAXS are the grain orientation and deformation produced by both the uniaxial stress and the resulting large strain of the disrupted areas. Mechanical properties of microcomposites (those of individual grains) and mechanical properties of macrocomposites (those of larger areas consisting of several grains dispersed in the disrupted material) should both be considered in the interpretation of the SAXS results. At first, strain-induced rotation of the nondisrupted stacks results from Le Chatelier's principle, that is, the selection of the lowest energy path of rearrangement of the macrocomposite in response to the uniaxial deformation of the material. At the beginning of the yield, the randomly oriented nondisrupted stacks are subjected to a shear process which causes their PS lamellae to rotate toward the stretching direction ($\chi \rightarrow 0$). However, opposed to this orientation is the increase of the Young's modulus of the grains with decreasing χ. In fact, as shown by Folkes and Keller,[15] the dependence of the Young's modulus of a lamellar grain composed of alternating layers of rubbery and rigid material on the angle χ between the lamellar surfaces and the stretching direction is given by

$$E_\chi = E_{90}(\sin^4\chi + 4\sin^2\chi\cos^2\chi)^{-1} \qquad (2)$$

where E_{90} is the Young's modulus transverse to the lamellar surfaces. Figure 6 shows the variation of E_χ/E_{90} as a function of χ according to eq 2. From this figure it is clear that E_χ/E_{90} increases abruptly at values of χ smaller than 20°. Thus it is suggested that the prevalent orientation of the grains observed at the beginning of the necking process is the result of two opposing effects: the shearing force due to the longitudinal extension together with the transverse contraction of the macrocomposite opposed by the increase of the tensile force of the latter due to the orientation of the microcomposite. In the first stage of the neck deformation, i.e., before the interlamellar shearing of individual grains, a slight decrease in the thickness of the rubbery lamellae is observed (see d_1 in Figure 5). This results from the transverse contraction of the specimen. The fact that the orientation angle χ is practically unchanged with further increase of the local strain is also a consequence of the abrupt increase of the grain Young's modulus with decreasing χ.

The second stage of the neck deformation is characterized by the interlamellar shearing of the individual

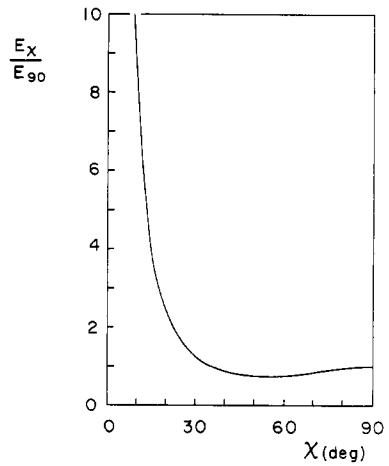

Figure 6. Variation of the Young's modulus ratio E_χ/E_{90} for a lamellar grain composed of alternating rubbery and rigid lamellae as a function of angle χ to the lamellar surfaces. Theoretical curve computed from eq 2 after Folkes and Keller.[15]

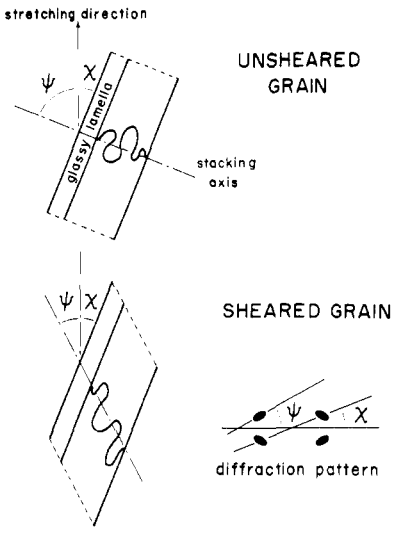

Figure 7. Schematic representation of the extension of a fictive rubbery chain along the stacking axis of a lamellar grain upon shearing of the glassy lamellae. Also represented is the angle ψ of the stacking axis with respect to the stretching direction together with its relationship with the orientation of the elongated lobes in the four-point SAXS pattern.

grains. This process which occurs at higher local strain ($\alpha_x > 1.4$) results from the selection of the lowest energy path of the microcomposite rearrangement in response to the higher local shear stress. Obviously, at these higher strains, interlamellar shearing of the individual grains requires less energy than more complete alignment of their lamellae along the stretching direction. Therefore, as α_x increases from 1.4 to 2.3 one observes a progressive but small change of lamellar orientation (χ decreases from 22 to 18°) with a concurrent substantial interlamellar shearing.

From the variation of the period d_1'' of the diffracting grains shown in Figure 5 it is clear that the deformation of the grains is not affine even at local draw ratio α_x as low as 1.2. In fact, at α_x values less than 1.4, d_1'' decreases slightly with increasing α_x. This indicates that the change in d_1'' resulting from the lateral contraction of the specimen is more important than that resulting from the macroscopic elongation. This behavior may be explained by considering, as before, that the grains are microcomposites which show a lower Young's modulus in the direction normal to their lamellar surfaces than in the parallel direction. Since the diffracting grains are oriented with their PS lamellae at an angle χ near 22° with respect to the stretching direction, they are therefore more easily deformable in the direction normal to the stretching direction than along this latter direction. Thus this feature of the microcomposite would account for the small decrease of d_1'' observed for α_x less than 1.4.

At α_x values greater than 1.4 the data in Figure 5 show a reverse trend in d_1'' which, as mentioned before, is associated with interlamellar shearing of the individual grains. Although the observed increase of d_1'' is small (d_1'' varies from 82 to 104 nm when α_x increases from 1.4 to 2.3), intragrain interlamellar shearing produces significant molecular extension in the rubbery lamellae. This effect results from the fact that each rubbery chain is anchored by its two ends at definite positions on the same or opposite PS lamella surfaces and becomes permanently entangled with the neighboring chains. Thus, when the rigid lamellae begin to slip one over the other, the rubbery chains tied on opposite PS lamellae (directly or through chain entanglements) become extended in a direction related to the shear strain direction. As illustrated in Figure 7, the extension of a fictive rubbery chain anchored at two points on a line normal to the lamellar surfaces in an initially unsheared grain can be described by the deformation of the rubbery lamella along the stacking axis of the grain. Indeed, if the latter is oriented at a known angle ψ with respect to the stretching direction, the molecular extension ratio α^*_ψ along the stacking axis of the grain can be estimated directly from ψ together with the lamellar orientation angle χ. Accounting for the thickness of the PS lamellae, which is given by $d_1^0\varphi_s$, where d_1^0 is the Bragg spacing d_1 measured before stretching and φ_s is the volume fraction of the PS microphase ($\varphi_s = 0.25$ in the present case), it can be shown that α^*_ψ is given by

$$\alpha^*_\psi = (d_1 - \varphi_s d_1^0)/[(1 - \varphi_s)d_1^0 \sin(\psi + \chi)] \quad (3)$$

Derivation of eq 3 is straightforward if one considers that $d_1^0 - \varphi_s d_1^0$ or $(1 - \varphi_s)d_1^0$ represents the end-to-end distance of the fictive chain in the unsheared grain before any stretching of the specimen and $(d_1 - \varphi_s d_1^0)/\sin(\psi + \chi)$ represents the end-to-end distance of the same chain in the sheared grain.

Table I
Comparison of Molecular Extension Ratio α^*_ψ along the Stacking Axis of the Grains with Macroscopic Draw Ratio $\alpha_{\theta=\psi}$ along the Same Direction

α_x	d_1, nm	χ, deg	ψ, deg	α^*_ψ eq 3	$\alpha_{\theta=\psi}$ eq 1
1.0	33.2				
1.2	31.4	22	58	0.94	0.97
1.4	30.8	22	48	0.96	1.00
1.8	30.8	21	27	1.22	1.27
2.3	30.8	17	16	1.66	1.69

As shown in Figure 7, ψ can be measured directly on the SAXS pattern, where it corresponds to the orientation of the elongated lobes with respect to the equator. Table I displays the values of d_1, χ, and ψ estimated from the first-order diffraction lobes recorded at $\alpha_x = 1.2$, 1.4, 1.8, and 2.3. Also listed in Table I are the values of α^*_ψ derived from eq 3. Inspection of the results shows that α^*_ψ increases from 0.94 to 1.66 when α_x increases from 1.2 to 2.3. In order to compare the molecular extension ratio α^*_ψ with the macroscopic deformation produced along the same direction as that of the stacking axis of the grains, we have calculated values of α_θ for $\theta = \psi$ using eq 1. These latter values are listed in the last column of Table I. Interestingly, they appear to be very close to those of α^*_ψ over the whole range of α_x measured in the neck region. This indicates that, despite the fact that the grain deformation does not follow the macroscopic deformation when one considers the variation of the period d_1'' measured along the stretching direction, the rubbery chain extension in the individual grains conforms closely to an affine behavior. That the grain deformation based on d_1'' does not show an affine behavior can be explained easily by considering that grains deform through shearing of the PS lamellae, a process which cannot be treated as a uniaxial tensile-strain deformation.

Concluding Remarks

In the present study, it has been shown that the structural changes associated with the neck deformation of the SBS-H lamellar system consist of a disruption process followed by orientation and shear of discrete lamellar grains at an angle close to 20° with respect to the stretching direction. Both the disruption and orientation processes seem to occur almost simultaneously at the outset of the yield while the shear process of the individual grains occurs later when larger local strain appears in the neck region.

The orientation and shear of the individual grains observed by SAXS have been explained by considering each grain as a microcomposite entity displaying a higher Young's modulus in the direction parallel to the lamellar surfaces than in the transverse direction. Our interpretation is that both these processes result from the selection of the lowest energy path of the grain rearrangement in response to the uniaxial macroscopic deformation of the material.

An interesting feature of the yielded material in the neck region is its isotropic constant-volume deformation behavior. This feature, which indicates a Poisson ratio close to 0.5 for the yielded material, suggests that the overall deformation results mainly from the rubbery microphase deformation with at best a minute amount only of ductile deformation of the glassy microphase. This clearly indicates that, already from the outset of the yield, the material can be considered as a dispersion of discrete lamellar grains in a rubbery matrix. Note that this feature is not a characteristic of the present morphology only. Recently, Odell and Keller[16] showed that extrusion-oriented SBS specimens consisting of hexagonally packed parallel PS rods in a PB matrix exhibited a Poisson ratio of 0.48 after being completely necked along the extrusion direction. In this latter case, as evidenced by electron microscopy, neck propagation resulted in the disruption of the PS rods in fragments 20–110-nm long which remained aligned with each other.

Another interesting feature of the yielded SBS-H lamellar system is the affine deformation of the rubbery chains observed in the oriented and sheared grains when the longitudinal macroscopic draw ratio increases from 1.2 to 2.3. Such affine behavior was also observed in the case of the extrusion-oriented SBS specimen ($w_s = 0.25$) studied by Odell and Keller[16] when stretched in the direction normal to the rod axis at draw ratios lower than 1.2. More recently, Hadziioannou et al.[17] reported a similar study on an oriented SIS specimen ($w_s = 0.30$) having rodlike morphology. They observed an affine behavior, i.e., a good agreement between macroscopic and lattice draw ratios, for macroscopic draw ratios ranging from 1 to 1.5, the latter being the largest draw ratio covered by their study.

As shown by the present study, solvent-cast three-block polymers having lamellar morphology together with a large volume fraction of rubbery microphase can recover readily their original structure characterized by randomly oriented lamellar grains when allowed to retract after stretching to draw ratios as great as 4, though the re-formation of grains with lamellae perpendicular to the stretching direction does not occur upon retraction. Excluding these latter grains, which seem to be those which are the more severely distorted during the neck deformation, it appears that the orientation and shear of the individual grains upon necking and further stretching are reversible processes. In this regard, there is a great similarity between solvent-cast three-block polymers of lamellar morphology and their analogues of rodlike morphology. In fact, Daniewska and Picot[9] in their study, which was based on small-angle light scattering measurements, showed that grains of parallel rods in solvent-cast SBS and SIS specimens underwent a reversible deformation upon stretching to draw ratios as great as 3.5. This reversibility indicates that the ruptured PS microphase tends to return to its original position and orientation when the stretched material is allowed to retract.

Acknowledgment. This work was supported by the Natural Sciences and Engineering Research Council of Canada and the Quebec Ministry of Education. We express our appreciation to Dr. T. L. Keelen of the Shell Development Co. for supplying the Kraton GX-6500 sample.

References and Notes

(1) Comprehensive reviews on SBS and SIS block polymers can be found in the following chapters: Dawkins, J. V. In "Block Copolymers"; Allport, D. C., Janes, W. H., Eds.; Wiley: New York, 1973; Chapter 8-B. Holden, J. In "Block and Graft Copolymerization"; Ceresa, R. J., Ed.; Wiley: New York, 1973; Vol. 1, Chapter 6. Noshay, A.; McGrath, J. E. "Block Copolymers, Overview and Critical Survey"; Academic Press: New York, 1977; Chapter 6.
(2) Fischer, E.; Henderson, J. F. *J. Polym. Sci., Part C* **1970**, *No. 30*, 459.
(3) Inoue, T.; Moritani, M.; Hashimoto, T.; Kawai, H. *Macromolecules* **1971**, *4*, 500.
(4) Pedemonte, E.; Alfonso, G. C. *Macromolecules* **1975**, *8*, 85.
(5) Hashimoto, T.; Fugimura, M.; Saijo, K.; Kawai, H.; Diamant, J.; Shen, M. *Adv. Chem. Ser.* **1979**, *No. 176*, 257.
(6) Bagrodia, S.; Wilkes, G. L. *J. Biomed. Mater. Res.* **1976**, *10*, 101.
(7) Séguéla, R.; Prud'homme, J. *Macromolecules* **1978**, *11*, 1007.
(8) Tarasov, S. G.; Tsvankin, D. Ya.; Godovskii, Yu. K. *Polym. Sci. USSR (Engl. Transl.)* **1979**, *20*, 1728.
(9) Daniewska, I.; Picot, C. *Polym. J.* **1978**, *10*, 141.
(10) Skoulios, A. E. In "Block and Graft Copolymers"; Burke, J. J., Weiss, V., Eds.; Syracuse University Press: Syracuse, N.Y., 1973; Chapter 7.
(11) Alexander, L. E. "X-Ray Diffraction Methods in Polymer Science"; Wiley-Interscience: New York, 1969; Chapter 5.
(12) Bonart, R.; Hosemann, R. *Kolloid-Z. Z. Polym.* **1962**, *186*, 16.
(13) Peterlin, A.; Baltá-Calleja, F. J. *J. Appl. Phys.* **1969**, *40*, 4238.
(14) Reinhold, C.; Fischer, E. W.; Peterlin, A. *J. Appl. Phys.* **1964**, *35*, 71.
(15) Folkes, M. J.; Keller, A. *Polymer* **1971**, *12*, 222.
(16) Odell, J. A.; Keller, A. *Polym. Eng. Sci.* **1977**, *17*, 544.
(17) Hadziioannou, G.; Mathis, A.; Skoulios, A. *Colloid Polym. Sci.* **1979**, *257*, 337.